One Single Static Measurement Predicts Wave Localization in Complex Structures

Gautier Lefebvre, Alexane Gondel, Marc Dubois, Michael Atlan, Florian Feppon, Aimé Labbé, Camille Gillot, Alix Garelli, Maxence Ernoult, Svitlana Mayboroda, et al.

One Single Static Measurement Predicts Wave Localization in Complex Structures

Gautier Lefebvre,[1] Alexane Gondel,[2] Marc Dubois,[1] Michael Atlan,[1] Florian Feppon,[3] Aimé Labbé,[3] Camille Gillot,[3] Alix Garelli,[3] Maxence Ernoult,[3] Svitlana Mayboroda,[4] Marcel Filoche,[3] and Patrick Sebbah[1,5,*]

[1]*Institut Langevin, CNRS, ESPCI Paris, PSL Research University, CNRS, 1 rue Jussieu, F-75005 Paris, France*

[2]*Mines Paris-Tech, 60 Boulevard Saint-Michel, F-75006 Paris, France*

[3]*Physique de la Matière Condensée, Ecole Polytechnique, CNRS, 91128 Palaiseau, France*

[4]*School of Mathematics, University of Minnesota, Minneapolis, Minnesota 55455, USA*

[5]*Department of Physics, The Jack and Pearl Resnick Institute for Advanced Technology, Bar-Ilan University, Ramat-Gan 5290002, Israel*

(Received 7 April 2016; published 10 August 2016)

A recent theoretical breakthrough has brought a new tool, called the *localization landscape*, for predicting the localization regions of vibration modes in complex or disordered systems. Here, we report on the first experiment which measures the localization landscape and demonstrates its predictive power. Holographic measurement of the static deformation under uniform load of a thin plate with complex geometry provides direct access to the landscape function. When put in vibration, this system shows modes precisely confined within the subregions delineated by the landscape function. Also the maxima of this function match the measured eigenfrequencies, while the minima of the valley network gives the frequencies at which modes become extended. This approach fully characterizes the low frequency spectrum of a complex structure from a single static measurement. It paves the way for controlling and engineering eigenmodes in any vibratory system, especially where a structural or microscopic description is not accessible.

DOI: 10.1103/PhysRevLett.117.074301

One of the key features exhibited by stationary waves in complex geometry or disordered systems is *localization*, characterized by an unexpected concentration of energy within a small portion of the system even in the absence of any confining potential [1]. Localization of waves may occur in the presence of structural or geometrical heterogeneities. A random potential, distributed scatterers, or specific boundary geometry can induce mode confinement under the right conditions [2]. Even the simplest geometry can produce localization, as was recently observed for mechanical vibrations in rigid plates with a single clamped point [3]. More complex geometries have demonstrated an efficient way to concentrate and dissipate energy in acoustical cavities [4,5], to tailor electromagnetic anechoic chambers [6], or to design musical instruments [7]. In nanophotonics, controlling light confinement is also an important challenge [8]. Indeed, the geometry of optical cavities and photonic crystals [9], as well as disordered structures [10], can be designed to optimize light trapping [11], miniaturize lasers [12], improve absorption efficiency of thin-film solar cells [13], store quantized bits of light [14], or modify spontaneous emission in cavity quantum electrodynamics [15,16]. Actually, in most cases, the investigation of localization is either based on empirical knowledge, numerical simulations, or optimization algorithms [17,18].

Being able to systematically predict the spatial and spectral characteristics of the confined modes—and to address the question of where the modes will localize—remains therefore a major challenge and often requires solving for a given geometry the full eigenvalue problem. In this Letter, we present a much simpler and more universal approach, taking advantage of landscape theory [19]. To this end, we design a test structure, a thin plate with complex geometry which exhibits localization of flexural waves. We show that the landscape function is a physical quantity directly accessible to the measure. Using laser holographic heterodyne technique, we measure the static deformation of the plate under uniform load, as well as its vibration modes. The "valley network" of the landscape precisely corresponds to the localization regions of the modes and the "hill peaks" give a good estimate of the corresponding resonance frequencies. Finally, the opening of the localization regions at higher frequencies is successfully predicted by the measured landscape as well and is confirmed by the observation of the transition from confined to extended modes. Because of the key information it contains, the landscape opens new perspectives in terms of measurements and the design of complex vibrating systems.

The system that we investigate is shown in Fig. 1. It consists of a 10 by 10 cm Duralumin square plate, 0.5 mm thick, with edges and different regions clamped, including an L-shape carved region, a segment, and two points. A detailed description of how the system is designed is provided in the Supplemental Material [20]. This geometry

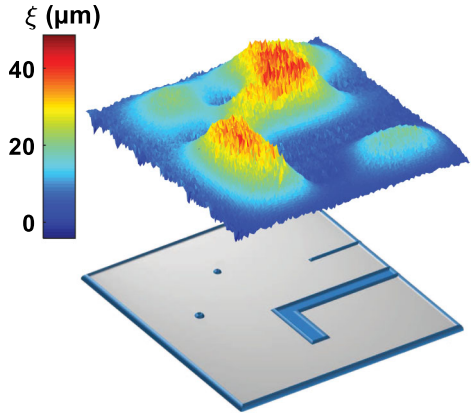

FIG. 1. The localization landscape. (Top panel) Absolute static deformation in μm of the 2D rigid thin plate under uniform pressure obtained by measuring the holographic phase map accumulated as pressure exerted on the plate is released (see movie 1 in the Supplemental Material [20]). (Bottom panel) Drawing of the 10×10 cm-large, 0.5 mm-thick metallic plate. The blue regions represent schematically the clamped regions: the edges, an L-shape carved region, a segment, and two points. The actual design of the system is detailed in the Supplemental Material [20]).

is inspired from the system studied in Ref. [19], where it was shown that its modal spatial distribution is highly nonintuitive, as it depends on the nature of the system (e.g., a rigid plate or a membrane) and, respectively, the associated canonical equation (bi-Laplacian or simple Laplacian).

We assume that the vibrating plate is thin compared to the wavelength, and that a local excitation results essentially in the creation of steady-state resonances of zeroth-order antisymmetric (A_0) Lamb waves, also called flexural waves in the low frequency regime. In that limit, the wave motion in an isotropic thin plate is well approximated by the Kirchhoff-Love equation [24]

$$\frac{\partial^2 w}{\partial t^2} + \frac{Eh^2}{12\rho(1-\nu^2)}\Delta^2 w = 0, \tag{1}$$

where $w(x,y)$ is the out-of-plane displacement, $h = 0.5$ mm is the plate thickness, and $E = 72.5$ GPa, $\rho = 2.79\ \mathrm{g\,cm^{-3}}$, and $\nu = 0.33$ are, respectively, the Young's modulus, the density, and the Poisson ratio of the material (here, Duralumin). The harmonic solutions of Eq. (1) take the form

$$w(x,y,t) = W(x,y)\exp(i\omega t). \tag{2}$$

The Rayleigh-Lamb dispersion relation of the A_0 mode in the low frequency approximation [24] relates the acoustic wave number k to the frequency ω:

$$k^2 = \alpha\omega, \quad \text{with} \quad \alpha = \sqrt{\frac{12\rho(1-\nu^2)}{Eh^2}}. \tag{3}$$

The eigenmodes of vibration W_m at the angular frequencies ω_m therefore satisfy the steady-state equation of flexural waves [25] derived from Eqs. (1), (2), and (3). The edges of the plate are clamped to be motionless, which results in a vanishing vibration amplitude and spatial derivative at the boundaries. Calling, respectively, Ω and $\partial\Omega$ the plate and its boundary, the mathematical formulation of the problem finally can be written

$$\begin{aligned} LW_m &= \omega_m^2 W_m \quad \text{on } \Omega, \\ W_m &= 0 \quad \text{on } \partial\Omega, \\ \partial_\nu W_m &= 0 \quad \text{on } \partial\Omega, \end{aligned} \tag{4}$$

where L is the elliptic operator

$$L = \frac{1}{\alpha^2}\Delta^2 \tag{5}$$

and ∂_ν is the normal derivative. According to the new localization theory proposed in Ref. [19], most of the information on flexural wave localization can in fact be retrieved from a mathematical object called the *localization landscape*. This object is a positive function $u(x,y)$ defined as

$$u(x,y) = \int_\Omega |G(x',y':x,y)|dx'dy', \tag{6}$$

where G stands for the Green function of the associated wave operator L. The landscape function controls the amplitude of the localized waves in the entire domain, which implies that the regions of low values of $u(x,y)$ are also the regions of small vibratory amplitude. In other words, the curves where u is small (referred to as the "valleys" hereafter) produce invisible barriers for waves. The propensity of the landscape u to constrain the amplitude of a steady-state vibration W_m emerges through the following inequality [19]:

$$|W_m(x,y)| \le \omega_m^2 u(x,y) \quad \forall\ (x,y) \in \Omega, \tag{7}$$

where W_m is normalized so that the maximal amplitude is equal to 1. Because of this specific choice of normalization, Eq. (7) corresponds to an actual constraint on the mode amplitude only at the points where $\omega_m^2 u(x,y) < 1$. In this picture, the valleys of u delimit the confining subregions for the localized eigenmodes. In summary, the partition of the plate created by these lines enables us to predict the subregions of the plate Ω where the vibrations will be localized.

The definition of u given in Eq. (6) makes it, in general, a complicated quantity to compute or to measure. However, if one assumes that the Green functions are positive everywhere (a property almost satisfied by the bi-Laplacian operator that we will discuss later in the Letter), then the absolute value can be removed in Eq. (6). In this case, u becomes the solution of the following Dirichlet problem:

$$\begin{aligned} Lu &= 1 \quad \text{on } \Omega, \\ u &= 0 \quad \text{on } \partial\Omega, \\ \partial_\nu u &= 0 \quad \text{on } \partial\Omega. \end{aligned} \tag{8}$$

In physical terms, the landscape u is thus the out-of-plane static deformation ξ under uniform load, modulo a multiplicative constant, that is,

$$u = \frac{\rho h}{P_0}\xi, \tag{9}$$

where P_0 is the applied pressure on the plate. This property has a very important consequence: it indicates that, without any computation or *a priori* knowledge of the system, the direct static measurement of ξ brings geometrical information about the localization subregions and quantitative information about the threshold above which delocalization will occur. This can prove particularly useful in disordered or random systems where the microscopic and structural information is lacking or unattainable.

To assess this conjecture, we measure the static deformation of the plate under uniform pressure, $P_0 = 4600$ Pa (as described in the Supplemental Material [20]) and we obtain the localization landscape shown in Figs. 1(a) and 2(a) (see also movie 1 in the Supplemental Material [20]). We can see the influence of the clamped regions on the landscape, constraining the amplitude of the deformation to remain smaller in their vicinity while other regions of the plate sustain a larger stretching. From this direct measurement, four local maxima are detected; hence, there are four localization subregions.

This measurement is compared to a numerical simulation of the landscape function solution of Eq. (8), computed using the finite element method (FEM) [26] and assuming a homogeneous medium [Fig. 2(b)]. The network of valleys is almost identical to the one measured (see the Supplemental Material [20]). It partitions the plate into the same four domains.

Using narrow-band and wide-field imaging heterodyne optical holography (see the Supplemental Material [20]) and scanning over frequency, we measure the spatial distribution of the out-of-plane vibration at resonance. The first eight modes are displayed in Fig. 3 and compared to FEM numerical simulations. The amplitude distribution of the measured eigenmodes appears very similar to the calculated vibration pattern at resonance.

The valley lines of the landscape are superimposed on each plot of Fig. 3. For a given frequency ω, only the portion of these lines where $\omega^2 u(x, y) < 1$ is plotted. Because of the normalization of the mode amplitude in Eq. (7), this subset of the valley lines is the only one exerting actual control on the mode amplitude [see Eq. (7)]. We observe that the first eigenmodes are confined within

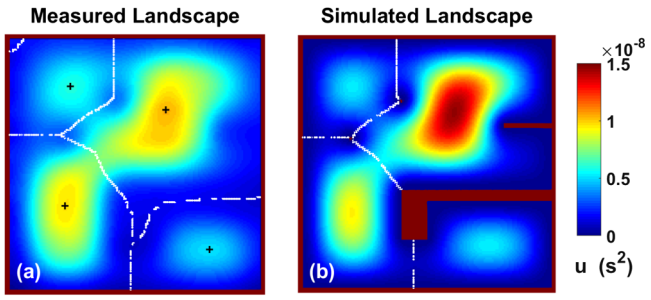

FIG. 2. Measured vs simulated landscape. (a) 2D representation of the measured landscape $u(x, y)$, issued from the plate static deformation shown in Fig. 1 after data processing (see the Supplemental Material [20]) and applying Eq. (9). The white lines are the watershed lines of steepest ascent or steepest descent that form the valley network of the landscape. The black crosses indicate the location of the local maxima of $u(x, y)$, from which the frequencies of the lower-spectrum localized modes are determined (see Fig. 4). (b) Calculated landscape using the finite element method to solve Eq. (8) for the same rigid plate as in the experiment.

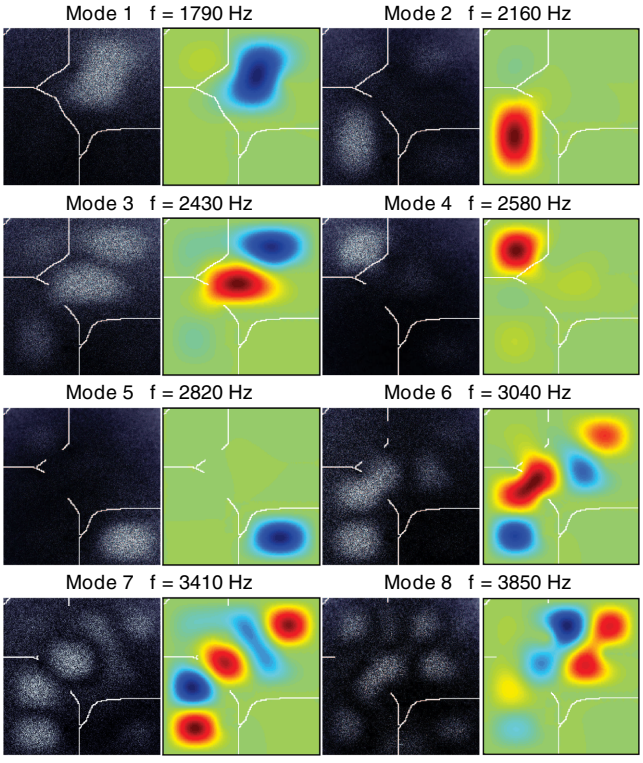

FIG. 3. Vibration modes. Local amplitude of flexural waves at the eight first resonances. Measurements (gray scale) using heterodyne holographic interferometry are compared side by side with a finite element method calculation (color scale) of the full elastic problem. Experiments and numerics give the same resonance frequencies up to mode 8. The superimposed white lines represent a subset of the valley network where $u(\vec{x}) \leq \omega^2$ and delimit the localization areas. As frequency increases, gaps open in the valley network and the modal confinement constraint is released.

the localization subregions predicted by a static measurement of the localization landscape. In fact, at low frequency, each eigenmode is almost an eigenfunction of one of the localization subregions.

Going further, the landscape provides not only spatial but also spectral information. Indeed, the resonance frequency of the fundamental mode in each subregion of the valley network can be extracted directly from the local maximum of the landscape function $u(x, y)$ in that particular subregion. We show in Ref. [20] that, theoretically, $\omega_i \simeq 1.27/\sqrt{\max_i(u)}$, where ω_i is the frequency of the fundamental mode (one single peak) in subregion i, and $\max_i(u)$ is the local maximum of u in the same region. This relation is confirmed experimentally by plotting in Fig. 4 the measured resonance frequencies of modes 1, 2, 4, and 5 vs the local maxima of the landscape function in the corresponding localization subregions. Remarkably, experimental points fit the theory within the error bars except for the first point (see the Supplemental Material [20]). A frequency estimate for higher order modes with two or more maxima is also possible, but it requires a more involved analysis. This is currently a work in progress [20]. The results presented here are the first step towards a prediction of the entire spectrum of vibratory systems from a simple static measurement.

As the frequency increases, the constraint expressed in Eq. (7) loosens, and gaps open along the valley lines (see movie 2 in the Supplemental Material [20]). As a result, initially isolated subregions become connected, meaning that modes can extend over larger domains. This is illustrated in Fig. 3 where, e.g., mode 2 remains confined while mode 3 brims over the small gap that is newly opened. Total mode delocalization over two subregions that were initially disconnected is observed, e.g., for mode 6. As the gaps widen, larger localization regions are formed and modes extend over the entire system. The frequency ω at which a gap opens along a valley line Γ satisfies $\omega^2 \max_\Gamma(u) = 1$, where the maximum of u is taken over Γ. This maximum is directly retrieved from the measured landscape function $u(x, y)$.

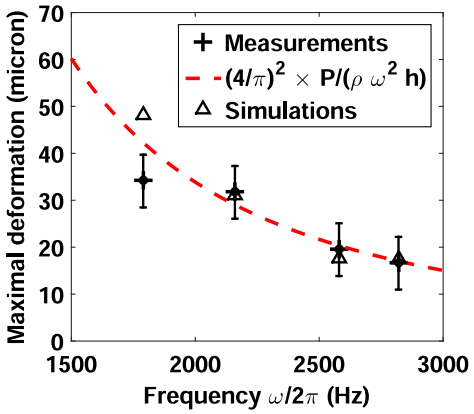

FIG. 4. Predicting the low frequency spectrum. (Crosses) Measured local maxima of the plate static deformation in each localization subregion (shown by crosses in Fig. 2) vs measured resonance frequencies of the first modes localized in the corresponding regions (modes 1, 2, 4, and 5 of Fig. 3. The error bars reproduce the uncertainty in the phase reference (see the Supplemental Material [20]). (Open triangles) The same information obtained from numerical simulations. (Dashed line) Theoretical prediction (see the Supplemental Material [20]).

We saw earlier that the positivity of the Green functions of the wave operator leads to Eq. (8)'s being satisfied by the landscape function. One has to point out that, in all generality, the bi-Laplacian with Dirichlet boundary conditions (vanishing amplitude and vanishing normal derivative) is not a positive operator. It means that the solution to a Dirichlet problem with positive load may change sign [27]. For example, it has been shown mathematically that the deformation of a square plate under uniform load exhibits an infinite number of smaller and smaller oscillations near the corners of the plate [28]. However, the amplitude of these alternating oscillations is so tiny that it is not measurable in a practical experiment. This is the case for most mechanical thin plates [29]. Thus, in practice, the solution to problem (8), obtainable from one static measurement only, is extremely close to the theoretical function defined in Eq. (6).

These results demonstrate experimentally the predictive nature of the landscape in a physical situation. The general behavior presented here shows that fundamental vibratory properties of the system are encoded in the landscape function, obtained from one static measurement. The landscape predicts the shape and location of the confining regions, as well as the frequencies of the localized low-energy modes. It also gives access to the value of the transition frequencies where the progressive coupling between neighboring regions eventually leads to a hybridization of their steady-state vibrations [30]. This is a first step in understanding the transition from a localized to an extended mode regime.

These results can be generalized to any disordered or structured system where the structural or microscopic information is not accessible, and therefore where no numerical solution of the localization landscape can be computed. They establish a strong and rigorous relationship between the static and dynamic properties of vibrating systems, independently of their dimensions or the nature of the vibrations. They further demonstrate how the landscape function can grant the experimentalists predictive power on the dynamical behavior of a system without having to force it or to solve the full modal problem. In the next step, the localization landscape should become a tool of choice for addressing the inverse problem, i.e., building the structure with desired spatial and frequency vibratory properties [31].

The authors thank Dominique Clément for the plate design and realization. P. S. is thankful for the Agence

Nationale de la Recherche support under ANR PLATON (Grant No. 12-BS09-003-01), the LABEX WIFI (the Laboratory of Excellence within the French Program Investments for the Future) under Grant No. ANR-10-IDEX-0001-02 PSL* and the PICS-ALAMO. This research was supported in part by The Israel Science Foundation (Grants No. 1781/15 and No. 2074/15). S. M. is partially supported by the Alfred P. Sloan Fellowship, the NSF CAREER Grant No. DMS-1056004, the NSF MRSEC Seed Grant DMR 0212302, and the NSF INSPIRE Grant DMS 1344235. M. F. is partially supported by a PEPS-PTI Grant from CNRS.

*patrick.sebbah@espci.fr

[1] P. W. Anderson, Absence of diffusion in certain random lattices, Phys. Rev. **109**, 1492 (1958).
[2] C. Even, S. Russ, V. Repain, P. Pieranski, and B. Sapoval, Localizations in Fractal Drums: An Experimental Study, Phys. Rev. Lett. **83**, 726 (1999).
[3] M. Filoche and S. Mayboroda, Strong Localization Induced by One Clamped Point in Thin Plate Vibrations, Phys. Rev. Lett. **103**, 254301 (2009).
[4] S. Félix, B. Sapoval, M. Filoche, and M. Asch, Enhanced wave absorption through irregular interfaces, Europhys. Lett. **85**, 14003 (2009).
[5] Colas Inc., Fractal Wall™, French Patent No. 0203404, U.S. Patent No. 10/508,119.
[6] L. H. Hemming, *Electromagnetic Anechoic Chambers: A Fundamental Design and Specification Guide* (Wiley-IEEE Press, New York, 2002).
[7] X. Boutillon and K. Ege, Vibroacoustics of the piano soundboard: Reduced models, mobility synthesis, and acoustical radiation regime, J. Sound Vib. **332**, 4261 (2013).
[8] K. J. Vahala, Optical microcavities, Nature (London) **424**, 839 (2003).
[9] Q. H. Song and H. Cao, Improving Optical Confinement in Nanostructures via External Mode Coupling, Phys. Rev. Lett. **105**, 053902 (2010).
[10] P. D. Garcia, R. Sapienza, C. Toninelli, C. Lopez, and D. S. Wiersma, Photonic crystals with controlled disorder, Phys. Rev. A **84**, 023813 (2011).
[11] B.-S Song, S. Noda, T. Asano, and Y. Akahane, Ultra-high-Q photonic double heterostructure nanocavity, Nat. Mater. **4**, 207 (2005).
[12] S. Noda, Seeking the ultimate nanolaser, Science **314**, 260 (2006).
[13] K. Vynck, M. Burresi, F. Riboli, and D. S. Wiersma, Photon management in two-dimensional disordered media, Nat. Mater. **11**, 1017 (2012).
[14] S. Lannebère and M. G. Silveirinha, Optical meta-atom for localization of light with quantized energy, Nat. Commun. **6**, 8766 (2015).
[15] L. Sapienza, H. Thyrrestrup, S. Stobbe, P. D. Garcia, S. Smolka, and P. Lodahl, Cavity quantum electrodynamics with Anderson-localized modes, Science **327**, 1352 (2010).
[16] R. Sapienza, P. Bondareff, R. Pierrat, B. Habert, R. Carminati, and N. F. van Hulst, Long-Tail Statistics of the Purcell Factor in Disordered Media Driven by Near-Field Interactions, Phys. Rev. Lett. **106**, 163902 (2011).
[17] A. P. Mosk, A. Lagendijk, G. Lerosey, and M. Fink, Controlling waves in space and time for imaging and focusing in complex media, Nat. Photonics **6**, 283 (2012).
[18] N. Bachelard, S. Gigan, X. Noblin, and P. Sebbah, Adaptive pumping for spectral control of random lasers, Nat. Phys. **10**, 426 (2014).
[19] M. Filoche and S. Mayboroda, Universal mechanism for Anderson and weak localization, Proc. Natl. Acad. Sci. U.S.A. **109**, 14761 (2012).
[20] See Supplemental Material at http://link.aps.org/supplemental/10.1103/PhysRevLett.117.074301, which includes Refs. [21–23], for more details on the experimental system, the measurement method of the vibration modes and localisation landscape function, the relation between the local maxima of the landscape function and the frequency of the localized modes, the numerical simulations, as well as links to two movies, one showing the measure of the localization landscape, the other one showing the opening of the valley network.
[21] A. Dillée, R. Cancilliere, F. Lopes, and M. Atlan, Video-rate computational heterodyne holography, Opt. Lett. **39**, 2090 (2014).
[22] F. Joud, F. Verpillat, F. Laloë, M. Atlan, J. Hare, and M. Gross, Fringe-free holographic measurements of large-amplitude vibrations, Opt. Lett. **34**, 3698 (2009).
[23] S. Timoshenko and S. Woinowsky-Krieger, *Theory of Plates and Shells* (McGraw-Hill, New York, 1959).
[24] D. Royer and E. Dieulesaint, *Elastic Waves in Solids* (Springer, Berlin, 2000), Vol. 1.
[25] L. N. Trefethen and T. Betcke, Computed eigenmodes of planar regions, Contemp. Math. **412**, 297 (2006).
[26] F. Hecht, O. Pironneau, A. Le Hyaric, and K. Ohtsuka, FREEFEM++ Manual, J. Numer. Math. **20**, 251 (2012).
[27] H.-C. Grunau and G. Sweers, In any dimension a "clamped plate", with uniform weight may change sign, Nonlinear Anal. Theory Methods Appl. **97**, 119 (2014).
[28] C. V. Coffman, On the structure of solutions to $\Delta^2 u = \lambda u$ which satisfy the clamped plate conditions on a right angle, SIAM J. Math. Anal. **13**, 746 (1982).
[29] F. Gazzola, H.-C. Grunau, and G. Sweers, *Polyharmonic Boundary Value Problems*, Lecture Notes in Mathematics Vol. 1991 (Springer-Verlag, Berlin, 2010).
[30] L. Labonté, C. Vanneste, and P. Sebbah, Localized mode hybridization by fine tuning of 2D random media, Opt. Lett. **37**, 1946 (2012).
[31] H. Benisty, Photonic crystals: New designs to confine light, Nat. Phys. **1**, 9 (2005).